Chemical Wave Packet Propagation, Reflection, and Spreading

Lingfa Yang and Irving R. Epstein*

Department of Chemistry and Center for Complex Systems, MS 015, Brandeis University, Waltham, Massachusetts 02454-9110

Received: May 8, 2002; In Final Form: July 10, 2002

Chemical waves can travel in well-defined packets. Two types of phase wave packets, distinguished by whether their component waves move toward or away from an initiating perturbation, are found in a reaction−diffusion model with a finite wave instability. Their propagation, reflection, and spreading are studied numerically and analytically. Reflection from a boundary or collision of two identical packets can result in standing waves. When two wave packets collide, they can interact briefly and then pass through each other without modification. The phase velocity, group velocity, and spreading velocity calculated by linear stability analysis with the inclusion of quadratic dispersion agree well with the results of numerical simulations.

1. Introduction

Wave packets in reaction−diffusion systems are rarely seen, even though wave packets have been intensively studied[1] in atomic, molecular, optical, and solid state physics, and also in laser chemistry. In those fields, manipulation or measurement of wave packet coherence is an important technique with potential applications to exploring the boundary between classical and quantum mechanics, controlling chemical reaction dynamics with lasers, and storing information in quantum computing or communication.

Wave packets in reaction−diffusion systems were first reported by Zhabotinsky et al.[2] in a model calculation, where the wave packet arises from a wave instability. The first experimental observation of wave packets in reaction−diffusion systems was made in the 1,4-cyclohexanedione Belousov−Zhabotinsky (CHD-BZ) system,[3] where the behavior was attributed to anomalous dispersion of the medium. Recently, wave packets were found in the BZ reaction in a reverse microemulsion (BZ-AOT) system[4,5] arising from a wave instability. Wave packets also occur in a differential flow system[6] due to convective instability.

A wave packet consists of waves whose wavenumbers lie in a small range, the so-called "narrowband". The packet is characterized by a width Δx in real space, and a mean wavenumber, k_0, in momentum space. The propagation is usually described by two velocities, the phase velocity, v_p, at which the component waves (carrier waves) move, and the group velocity, v_g, at which the peak of the wave packet travels. The concept of group velocity appears to have been first enunciated by Hamilton[7] in 1839. A group velocity can be positive or negative. A negative group velocity implies that the individual waves move in a direction opposite to that of the packet as a whole. Such a phenomenon was first pointed out in 1904 as a consequence of anomalous (negative) dispersion[8] and has been of interest recently in connection with superluminal light.[9]

The spreading of the wave packet depends on the medium through which it propagates. A packet, which represents the Green function of an initially localized impulse perturbation, is stable if it asymptotically decays in any uniformly translating frame. Otherwise, the packet is unstable. An unstable packet is absolutely unstable if, at any fixed location, the waves' amplitude grows in time. It is convectively unstable if the amplitude decays at all points in a fixed frame but grows in some moving frame.[10]

In this paper, we study wave packets in a homogeneous reaction−diffusion model. We call these chemical wave packets, because the waves consist of concentrations varying in space and are generated by a wave instability arising from the interplay of chemical reaction and diffusive transport. In homogeneous reaction−diffusion systems, traveling waves, resulting from excitability or a Hopf bifurcation, usually occur as wave trains, as in the case of the familiar spiral waves and target patterns. In contrast to wave packets, which move in space and occupy a finite region, wave trains continue indefinitely (in principle) to emerge from a fixed source and to expand. We find that chemical waves can travel in well-defined packets when the wave instability is present. From an initially localized impulse perturbation, the wave instability gives rise to packets that always move outward, away from the initial perturbation. The component waves, however, can propagate either outward or inward. Outwardly propagating (OP) waves are more common; inwardly propagating (IP) waves are rarely seen. IP wave packets are also referred to as backward volume waves (BVW).[11] One special feature we find for these chemical wave packets is that two packets can pass through each other like solitons, rather than annihilating as in the case of spiral waves.

2. Phase Velocity, Group Velocity, and Speed of Spreading of a Wave Packet

The wave instability plays an important role in pattern formation in many systems, such as binary fluid convection,[12] surface reactions,[13] electrochemical reactions,[14] and the BZ-AOT system.[4] When a wave instability emerges in a homogeneous reaction−diffusion system, the symmetry of the uniform steady state solution is broken, generating oscillatory patterns periodic both in time (oscillatory frequency $\omega_c \neq 0$) and in space (wavenumber $k_c \neq 0$).[12]

Just above the wave bifurcation, a small perturbation can cause the system to leave the steady state, producing waves

* To whom correspondence should be addressed. E-mail: epstein@brandeis.edu.

Wave Packet Propagation, Reflection, and Spreading

J. Phys. Chem. A, Vol. 106, No. 47, 2002 **11677**

with wavenumbers lying within a narrowband around the characteristic wavenumber k_c. Superposition of waves in the narrowband results in amplitude modulation and may form wave packets. For simplicity, we take as an example two waves with slightly different wavenumbers $k_1 = k_c - \Delta k$ and $k_2 = k_c + \Delta k$. The corresponding frequencies are $\omega_1 = \omega(k_c) - \Delta\omega$ and $\omega_2 = \omega(k_c) + \Delta\omega$. The superposition gives

$$A(x, t) = A_1(x, t) + A_2(x, t) = A_0 \cos[(k_c - \Delta k)x - (\omega - \Delta\omega)t] + A_0 \cos[(k_c + \Delta k)x - (\omega + \Delta\omega)t] = 2A_0 \cos(k_c x - \omega t) \cos(\Delta k_c x - \Delta\omega t) \quad (1)$$

Because $k_c \gg \Delta k$, the term $\cos(\Delta k_c x - \Delta\omega t)$ in eq 1 can be regarded as a modulation of the $\cos(k_c x - \omega t)$ (plane wave) term. The phase velocity of the plane waves is then

$$v_p = \frac{\omega(k)}{k}\Big|_{k=k_c} \quad (2)$$

and the velocity of the packet (group velocity) is $v_g = \Delta\omega(k)/\Delta k$. As $\Delta k \to 0$ and $k \to k_c$, we have

$$v_g = \frac{d\omega(k)}{dk}\Big|_{k=k_c} \quad (3)$$

The spreading of a wave packet is due to the dependence of the phase velocity on the wavenumber.

$$v_g = v_p + k\frac{dv_p}{dk} \quad (4)$$

On the basis of the sign of dv_p/dk, three types of media are possible as follows: normal dispersive ($dv_p/dk < 0$), nondispersive ($dv_p/dk = 0$), and anomalous ($dv_p/dk > 0$). The group velocity describes the motion of the point of maximum amplitude in the packet. For a quantum particle wave, it equals the speed of the particle,[15] with which the energy in the group is transmitted. In normal media, $dv_p/dk < 0$, which implies $v_g \leq v_p$; in nondispersive media, for example, light in a vacuum with constant velocity c, we have $v_g = v_p$; in anomalous dispersion, $v_g > v_p$. Superluminal (faster than c) light has been reported due to anomalous dispersion.[9]

A wave packet centered around the wavenumber k_c can be written as the inverse Fourier transform

$$\Psi(x, t) = \int_{-\infty}^{+\infty} g(k - k_c) e^{i(kx - \omega t)} \, dk \quad (5)$$

where $g(k) = \int_{-\infty}^{+\infty} G(x) e^{-ikx} \, dx = (8\pi\sigma^2)^{1/4} e^{-k^2\sigma^2}$ is the Fourier transform of the Gaussian function, $G(x) = (2\pi\sigma^2)^{-1/4} e^{-x^2/4\sigma^2}$ with a root-mean-square (rms) width $\Delta x = \sigma$. A wave packet in general involves a band of waves centered around the characteristic wavenumber k_c. We take the Taylor series expansion of ω in the narrowband $\Delta k = k - k_c$

$$\omega = \omega_0 + (k - k_c)\alpha + \frac{1}{2}(k - k_c)^2\beta + o(k - k_c)^3 \quad (6)$$

where $\alpha = d\omega/dk = v_g$ and $\beta = d^2\omega/dk^2$. For linear dispersion, only the first two terms in the expansion are considered. Here,
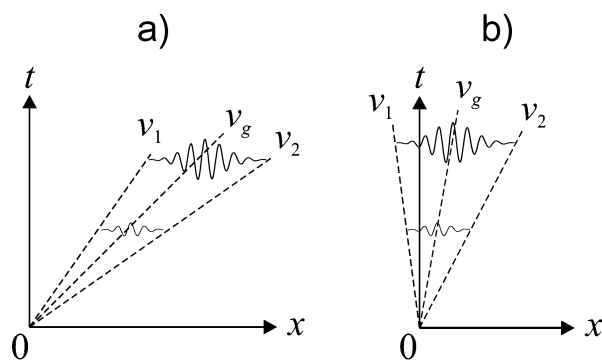

Figure 1. Schematic plots showing a linearly convectively unstable (growing amplitude) packet with a large group velocity (a) and a linearly absolutely unstable packet with a small group velocity giving a wave train (b).

we include the third term (quadratic dispersion)

$$\Psi(x, t) = \int_{-\infty}^{+\infty} g(k - k_c) e^{i(kx - \omega t)} \, dk$$
$$= \int_{-\infty}^{+\infty} (8\pi\sigma^2)^{1/4} e^{-k^2\sigma^2} \times$$
$$e^{i[(k+k_c)x - \omega_0 t - \alpha(k-k_c)t - (1/2)\beta(k-k_c)^2 t]} \, dk$$
$$= e^{i(k_c x - \omega_0 t)}(8\pi\sigma^2)^{1/4} [\pi/(\sigma^2 + i\beta t/2)]^{1/2} \times$$
$$e^{-(x-\alpha t)^2/4(\sigma^2 + i\beta t/2)} \quad (7)$$

At time t, the packet is centered at $x(t) = x(0) + |v_g|t$, and its rms width, from the real part of the exponential function in eq 7, is

$$\Delta x(t) = \sqrt{\sigma^2 + \left(\frac{\beta t}{2\sigma}\right)^2} \quad (8)$$

Thus, for sufficiently long times, the rms width of the packet increases linearly with time.

A wave packet emanating from an initial disturbance may evolve as an isolated packet, as a wave train, or even as a standing wave, depending upon the magnitude of the group velocity, $|v_g|$. If $|v_g|$ is large relative to the speed of packet spreading, $\beta/2\sigma$, given by eq 8, an isolated packet leaves the site of the initial pulse perturbation (the source) quickly, and the initial perturbation dies away (Figure 1a). If $|v_g|$ is slower than the spreading of the packet, the packet tail moves backward, toward the source, resulting in continued local oscillation in the region between the source and the outermost edge of the packet (Figure 1b). In effect, the initial perturbation remains as a source of waves, creating a wave train rather than a wave packet. If $|v_g| = 0$, the center of the wave packet remains at the source, producing waves of equal amplitude in both directions, which can interact to form standing waves:

$$A(x, t) = A_0 \cos(kx - \omega t) + A_0 \cos(kx + \omega t) = 2A_0 \cos(kx) \cos(\omega t) \quad (9)$$

When the length of the system satisfies $L = n\pi/k$, where n is an integer, standing waves appear with stationary nodes at $x = m\pi/k$, $m = 0, 1, ..., n$.

3. Reaction−Diffusion Model

To study the behavior of chemical wave packets, we constructed a reaction−diffusion model based on the following

abstract scheme:

$$A \xrightarrow{k_1} X + P \tag{10}$$

$$B + X \xrightarrow{k_2} Y + D \tag{11}$$

$$2X + Y \xrightarrow{k_3} 3X \tag{12}$$

$$X \xrightarrow{k_4} E \tag{13}$$

$$X \xrightarrow{k_f} Z \tag{14}$$

$$Z \xrightarrow{k_b} X \tag{15}$$

Reactions 10−13 constitute the well-known Brusselator model.[16] The additional steps 14 and 15 describe a reversible interconversion between the activator (X) and an unreactive form (Z). This interconversion may arise, for example, in the BZ-AOT system, from transfer of the activator from one phase (aqueous) to another (oil), where it is unreactive because of the absence of reaction partners.[5]

From reactions 10−15, we obtain three partial differential equations:

$$\frac{\partial u}{\partial t} = D_u \nabla^2 u + f(u, v) - (cu - dw) \tag{16}$$

$$\frac{\partial v}{\partial t} = D_v \nabla^2 v + g(u, v) \tag{17}$$

$$\frac{\partial w}{\partial t} = D_w \nabla^2 w + (cu - dw) \tag{18}$$

where the variables u, v, and w are the dimensionless concentrations of the activator (X), inhibitor (Y), and "inactivator" (Z), whose corresponding diffusion coefficients are D_u, D_v, and D_w, respectively. The parameters c and d are rescaled[17] from the rate constants k_f and k_b. The Brusselator kinetics[16] are given by the functions f and g as

$$f(u, v) = a - (1 + b)u + u^2 v \tag{19}$$

$$g(u, v) = bu - u^2 v \tag{20}$$

The steady state of the model (16−18) is at $(u_{ss}, v_{ss}, w_{ss}) = (a, b/a, ac/d)$. Linear stability analysis around this steady state yields the characteristic equation for the eigenvalues λ. Of the three eigenvalues, we may have either one real and one complex conjugate pair or three real. We are interested in the complex pair. The finite wave instability occurs when $Re(\lambda) = 0$ at $k = k_c \neq 0$, and $Re(\lambda) < 0$ for all other k. This may happen when the diffusion coefficients are such that $D_u < D_v \ll D_w$, a case that arises in the BZ-AOT system, where nanometer-sized water droplets are dispersed in a continuous oil phase. The droplets carrying the activator, HBrO$_2$, diffuse much more slowly (10^{-7} cm^2/s level) than do small molecules such as the inactivator, BrO$_2$, in the oil phase (10^{-5} cm^2/s level).[4]

4. Results of Simulations

A. Simulations and Calculations for an IP Wave Packet. Figure 2 illustrates an IP wave packet. The parameters were chosen so that the finite wave instability was close to the onset point ($Re(\lambda) = 0^+$, at $k = k_c$). The system was initialized to the homogeneous steady state. At $t = 0$, we applied a narrow spike
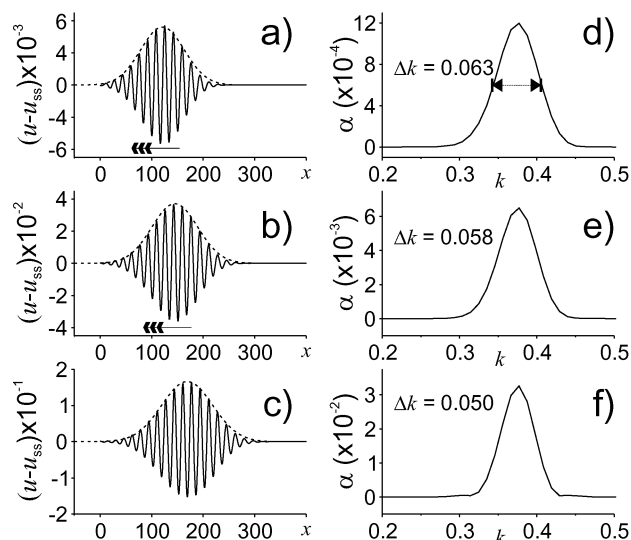

Figure 2. One-dimensional simulation of IP wave packet. The packet moves to the right, while individual waves propagate to the left as shown by the arrow. Parameters $(a, b) = (3, 11.39)$, $c = d = 1$, $D = (0.5, 1, 20)$. Initial perturbation at $x = 0$, $t = 0$. Snapshots were taken at $t = 500$ (a), 600 (b), and 700 (c). Packet envelope was fitted by a Gaussian function (dashed line). Center position and width are $x = 121, 145, 169$ and $\sigma = 60, 63, 70$. Corresponding Fourier spectra plotted in panels d−f have widths $\Delta k = 0.063, 0.058, 0.050$.

perturbation to the variable u. The Fourier spectrum of such a perturbation contains an abundance of wavenumbers. Because of the finite wavelength instability, waves within a narrowband around $k = k_c$ can grow; outside of this narrowband, waves are suppressed. A local oscillation is induced around the center of the initial perturbation ($x = 0$) but damps out because the Hopf mode is below onset ($Re(\lambda) < 0$, at $k = 0$). A wave packet then forms in which the profile of the inner waves is sinusoidal and the amplitude is modulated by a Gaussian-like function (Figure 2).

The wave packet slowly moves outward as new waves are formed, while the individual waves within the packet move much more rapidly toward the site of the original perturbation. We measured these two speeds in our simulations. At each moment, we fit the envelope with a Gaussian function. The movement of the maximum point gives the group velocity $|v_g| = 0.24$ (Figure 2a−c). To find the phase velocity, we recorded snapshots and constructed space−time plots, which yielded $v_p = 10.53$.

It is also possible to calculate the wave speed from the dispersion relation. The results of our linear stability analysis are shown in Figure 3. The real part of the most positive eigenvalue is plotted in Figure 3a, where the finite wave instability is seen at $k_c = 0.376$, which is very close to onset. The corresponding imaginary part, which decreases monotonically, is shown in Figure 3b; its derivative appears in Figure 3c, where the group velocity is found to be $v_g = -0.24$ at $k = k_c$. The negative sign for v_g implies that the component waves propagate inward, toward the "source". The second derivative plotted in Figure 3d is related to the spreading of the packet envelope (eq 8). Figure 3e shows ω/k calculated from the data in Figure 3b, enabling us to read off the phase velocity as $v_p = 10.53$. The derivative of the phase velocity (Figure 3f) determines the dispersion of the medium through which the waves propagate (eq 4).

From the simulation in Figure 2, we can clearly see that the wave packet becomes broader with time. This effect results from dispersion, i.e., from the dependence of the phase velocity on
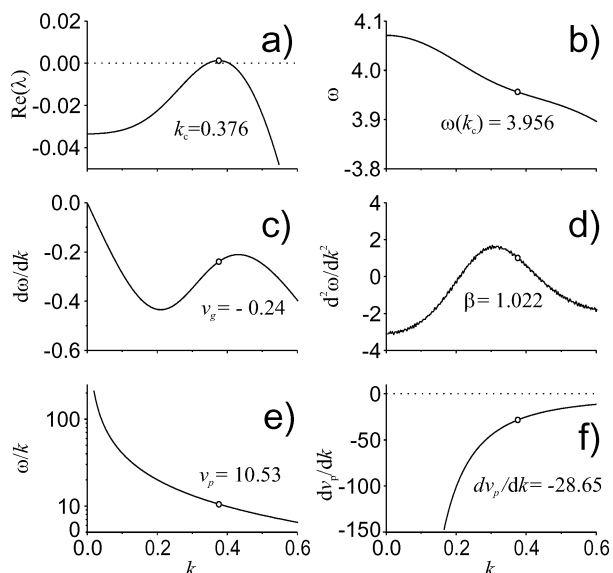
Wave Packet Propagation, Reflection, and Spreading

J. Phys. Chem. A, Vol. 106, No. 47, 2002 **11679**

Figure 3. Dispersion curves showing real (a) and imaginary (b) parts of the complex eigenvalue at the homogeneous steady state of the model (16−18) (see Figure 2 for parameters). Finite wave instability appears in panel a, and the corresponding imaginary part decreases monotonically in panel b, resulting in negative first derivative (group velocity) in panel c. The second derivative in panel d is related to dispersion in velocity. Phase velocity $v_p = \omega/k$ is shown in panel e, with its first derivative, which is related to the dispersion of the medium, in panel f. Values at k_c are marked with small circles.
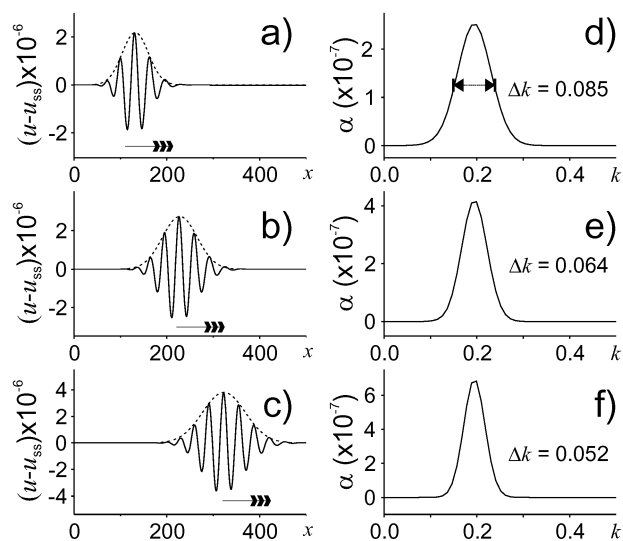

Figure 4. One-dimensional simulation of OP wave packet. The packet center and individual waves both propagate to the right as shown by the arrow. Parameters $(a, b) = (1, 2.9)$, others as in Figure 2. Initial perturbation at $(x, t) = (0, 0)$. Snapshots were taken at $t = 140$ (a), 240 (b), and 340 (c). The packet envelope was fitted by a Gaussian function (dashed line). The center position and width are $x = 132$, 228, 323 and $\sigma = 40$, 53, 65. Corresponding Fourier spectra plotted in panels d−f have widths $\Delta k = 0.085$, 0.064, 0.052.

wavenumber. In our calculation in Figure 3f, we have $dv_p/dk = -28.65$, which results in $v_g = v_p + k(dv_p/dk) = -0.24$. This negative group velocity is responsible for our IP wave packet. As the packet's width increases in coordinate space, its width in momentum space shrinks according to the "uncertainty principle" $\Delta x \Delta k \geq 2\pi$ (Figure 2).

B. Simulations and Calculations for an OP Wave Packet. Simulations of OP wave packets are presented in Figure 4, and the results of linear stability analysis are presented in Figure 5.
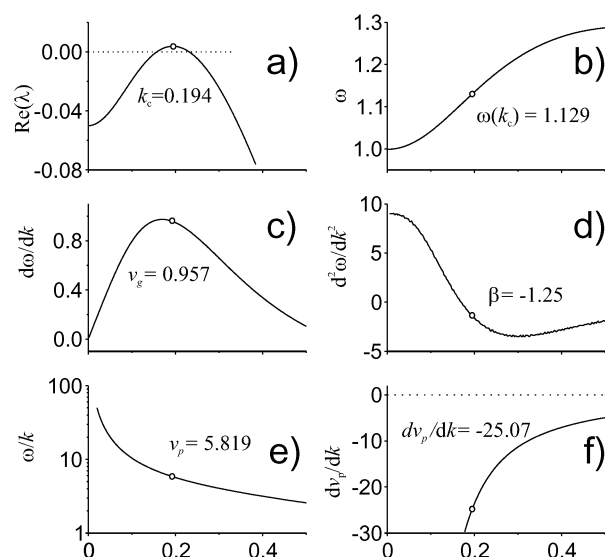

Figure 5. Dispersion curves showing real (a) and imaginary (b) parts of the complex eigenvalue at the homogeneous steady state of the model (16−18) (see Figure 4 for parameters). See Figure 3 for description of panels a−f.

When an OP packet is generated by a perturbation, the individual waves propagate outwardly, as does the packet as a whole (Figure 4a−c). OP packets contain fewer waves than IP packets, because the wavenumber here is smaller than in the IP case (compare k_c in Figure 3a and Figure 5a). Again, the phase and group velocities obtained in the simulations are in excellent agreement with the results of the linear stability analysis.

C. Reflection and Passing through of Wave Packets. When a wave packet reaches the zero-flux boundary, reflection occurs. The OP wave packet simulation of Figure 4 is continued in Figure 6. When $t = 625$, the OP packet reaches the right boundary (Figure 6a), and "bounces off" the "wall", changing the sign of both the phase and the group velocities. During reflection, the incident left-moving waves interact with the reflected right-moving waves to form transient standing waves (Figure 6d).

Figure 6b shows another simulation in which two packets, one from the left, the other from the right, collide at $t = 310$, are reflected at $t = 2 \times 310$, and then collide again at $t = 3 \times 310$. Both collision and reflection lead to the appearance of standing waves due to interaction between waves from opposite directions.

Figure 6b raises the question whether, when two waves meet, they "pass through" or "bounce off" each other. If wave packets behave as particles, they should bounce off. Because the two packets in Figure 6b are identical except for their direction of propagation, we cannot distinguish between these possibilities.

To answer this question, we carried out a third simulation (Figure 6c), where one packet was initialized at $t = 0$ and a second one started at $t = 240$. When they meet at $t = 450$, the first packet is significantly wider than the second. When the packets separate, we recognize that they pass through one another without any apparent deformation after they separate. We conclude that when the two identical packets in Figure 6b collide, they, too, pass through each other unaffected by the collision.

We also studied the collision of IP wave packets. They behave the same as OP packets in this respect, because both IP and OP packets consist of phase waves, and both are generated from a wave instability.
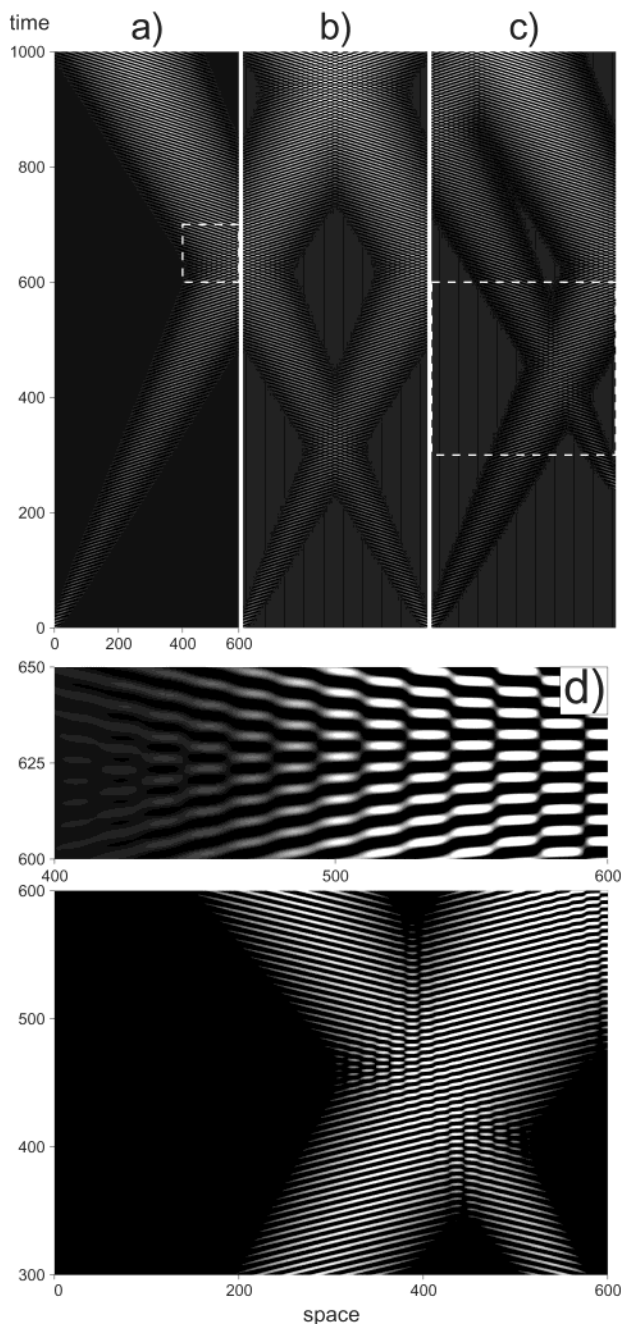
Figure 6. Reflection and collision of wave packets. (a) Reflection of single wave packet from boundary at $t \approx 600$. (b) Two symmetric packets meet before and after reflection at $t \approx 600$. (c) Two nonsymmetric packets meet at $t \approx 400$ and pass through each other. (d) Standing waves during reflection from boundary (zoom of box in panel a. (e) Zoom of interacting waves in box from panel c.

D. Wave Trains and Standing Waves. Both the OP and the IP wave packets analyzed above have relatively large absolute group velocities, $|v_g|$, as compared with the speed of packet spreading, so that we see well-defined packets moving away from the initial perturbation or source, which soon dies out. This situation was shown schematically in Figure 1a, where the packet is linearly convectively unstable. If $|v_g|$ is less than a critical value, the tail of the packet extends backward, which results in the local oscillation amplitude increasing everywhere. Such a packet is linearly absolutely unstable (Figure 1b).

The simulations in Figure 7 are carried out with zero-flux boundary conditions just above the wave instability bifurcation line in the (a, b) parameter plane. An initial perturbation is added

at the left end, while the rest of the system is placed in the uniform steady state. With relative large $|v_g|$ (Figure 7a,e), packets leave the source at $x = 0$ and quickly move to the right. At $|v_g| = 0$ (Figure 7c), the center of the wave packet remains at the source, the component waves are reflected by the left boundary and interact with the incoming waves of the same amplitude to form standing waves. When $|v_g|$ is small (Figure 7b,d), we have an absolute instability. Now the component waves reflect, but they are weaker than the incoming waves, and the interaction results in a train of traveling waves modulated by standing waves near the source.

5. Conclusion and Discussion

We have studied here the propagation, reflection, and spreading of chemical wave packets. We found that chemical wave packets behave in much the same way as physical wave packets.

When a uniform reaction−diffusion system is subjected to a perturbation, the pure finite wave instability ($Re(\lambda) = 0^+$ at $k = k_c$) can give rise to wave packets. These packets always move outward from the perturbation, but the component waves can propagate inward or outward, depending upon the sign of the group velocity.

The propagation of waves in packets requires that the absolute value of the group velocity, $|v_g|$, be sufficiently large as compared with the speed of packet spreading. Standing waves appear when $|v_g| = 0$, and trains of traveling waves occur when $|v_g|$ is small.

The component waves of both OP and IP wave packets resemble the phase waves seen, for example, in spatially extended oscillating reactions in the presence of a concentration gradient−their amplitudes are small, and their wave profiles are sinusoidal. These features distinguish them from trigger waves, whose amplitudes are much larger and whose profiles are sharp and are typically followed by a long refractory "tail".

The generally accepted wisdom that chemical waves cannot pass through or bounce off one another applies only to trigger waves in excitable media and not to phase wave packets. This is another clear difference between trigger and phase wave packets. For trigger waves in excitable systems, when two wave fronts meet, they annihilate due to their accompanying refractory regions, and the refractory zone thus produced does not support wave propagation until it has recovered its excitability. Phase wave packets do not have such a refractory region. They can reflect from zero-flux boundaries or pass through each other, like solitons, after experiencing transient interference in the region where they overlap.

One may ask why chemical wave packets are so rarely encountered in experiments and whether there are reaction−diffusion systems in which wave packets are likely to be found. Although wave packets can occur in special situations involving anomalous dispersion[3] or flows,[6] it appears that the most promising source of this behavior involves the wave instability. Systems possessing a wave instability must necessarily have a minimum of three independent variables and a significant spread of diffusion coefficients. These requirements are fulfilled by the BZ-AOT system.[5] Other promising classes of systems, in which multiple species with potentially quite different diffusion constants are involved in the dynamics, include catalytic reactions such as the oxidation of carbon monoxide on single crystals of platinum[13] and electrochemical reactions.[14] One must take care to work under conditions where the uniform steady state is stable to homogeneous perturbations, because if there is also a Hopf instability, sustained oscillations will create a
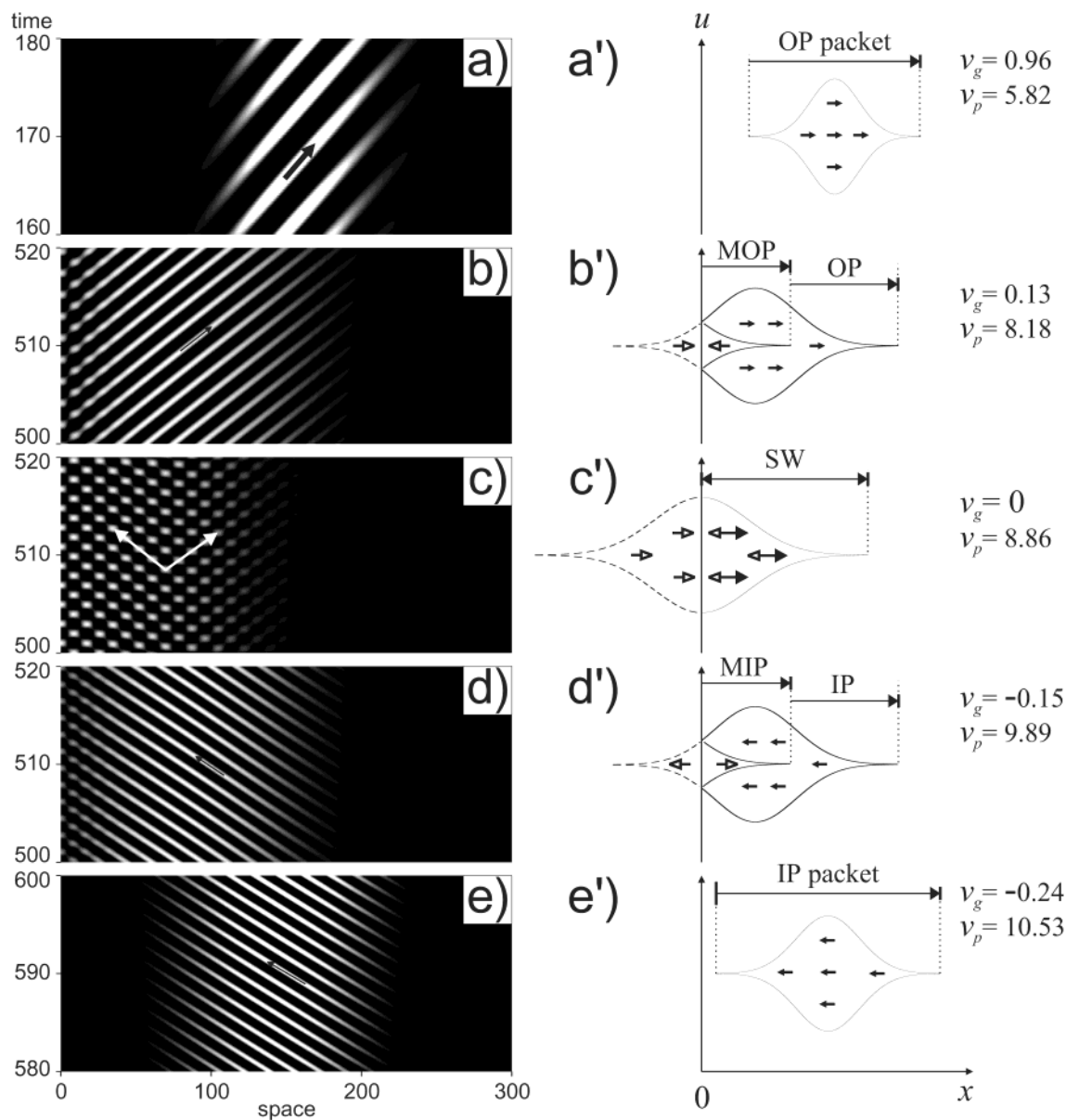
Figure 7. Typical spatial−temporal patterns along the transition from OP to IP waves. (a) OP wave packet, (b) modulated OP traveling waves, (c) standing waves (d) modulated IP traveling waves, and (e) IP wave packet. Waves' propagation direction (OP/IP) is marked with an arrow. Standing waves are marked with two arrows for OP and IP wave components. Each frame comprises 20 time units. Diffusion coefficients $D = (0.5, 1, 20)$, and rates $c = d = 1$ in all panels. Variable parameters are $(a, b) = (1.0, 2.9)$ (a), $(2.2, 7.1)$ (b), $(2.46, 8.37)$ (c), $(2.8, 10.2)$ (d), and $(3.0, 11.39)$ (e). Schematic plots corresponding to each wave packet on the right show Gaussian type envelopes, which form a spindle. The height corresponds to the amplitude of the component waves. The segments at $x < 0$ (dashed envelope) are virtual (mirror) waves due to the zero-flux boundary condition at $x = 0$. Arrows inside the spindles show propagation direction of the component waves, while open arrows show directions of mirror waves. All packets move to the right with group velocity $|v_g|$. MOP (MIP) = modulated outwardly (inwardly) propagating; SW = standing waves.

wave train, destroying the packet behavior. Finally, it is important to carry out the experiments not too far beyond the onset of the wave bifurcation in order to avoid, on one hand, initiation of trigger waves that may annihilate the phase wave packets, and, on the other, having too broad a range of unstable wavenumbers to satisfy the narrowband condition for wave packet formation. Given these multiple constraints, it is understandable that sightings of chemical wave packets have been so infrequent to date.

References and Notes

   (1) Yeazell, J. A., Uzer, T., Eds.; *The Physics and Chemistry of Wave Packets*; Wiley: New York, 2000.

   (2) Zhabotinsky, A. M.; Dolnik, M.; Epstein, I. R. *J. Chem. Phys.* **1995**, *103*, 10306.

   (3) (a) Manz, N.; Muller, S. C.; Steinbock, O. *J. Phys. Chem. A* **2000**, *104*, 5895. (b) Hamik, C. T.; Manz, N.; Steinbock, O. *J. Phys. Chem. A* **2001**, *105*, 6144.

   (4) Vanag, V. K.; Epstein, I. R. *Science* **2001**, *294*, 835; *Phys. Rev. Lett.* **2001**, *87*, 8301.

   (5) Vanag, V. K.; Epstein, I. R. *Phys. Rev. Lett.* **2002**, *88*, 8303.

   (6) Satnoianu, R. A.; Merkin, J. H.; Scott, S. K. *Chem. Eng. Sci.* **2000**, *55*, 461.

   (7) Hamilton, W. R. *Proc. R. Irish Acad. 1* **1839**, *267*, 341; *The Propagation of Disturbances in Dispersive Media*; Havelock, T. H., Ed.; Cambridge Press: Cambridge, 1914.

(8) Lamb, H. *Proc. London Math. Soc.* **1904**, *1*, 473.

(9) Wang, L. J.; Kuzmich, A.; Dogariu, A. *Nature* **2000**, *406*, 277.

(10) Couairon, A.; Chomaz, J.-M. *Physica D* **1997**, *108*, 236.

(11) Kovshikov, N. G.; Kalinikos, B. A.; Patton, C. E.; Wright, E. S.; Nash, J. M. *Phys. Rev. B* **1996**, *54*, 15210.

(12) Cross, M. C.; Hohenberg, P. C. *Rev. Mod. Phys.* **1993**, *65*, 851.

(13) (a) Jakubith, S.; Rotermund, H.; Engel, W.; Oertzen, A. v.; Ertl, G. *Phys. Rev. Lett.* **1990**, *65*, 3013. (b) Imbihl, R.; Ertl, G. *Chem. Rev.* **1995**, *95*, 697.

(14) (a) Lev, O.; Sheintuch, M.; Pisemen, L. M.; Yanitzky, C. *Nature* **1988**, *336*, 458. (b) Krischer, K.; Mazouz, N.; Grauel, P. *Angew. Chem., Int. Ed.* **2001**, *40*, 850.

(15) For a nonrelativistic particle, $E = \hbar\omega$ and $p = \hbar k$. This gives $v_{\mathrm{p}} = \omega/k = E/p = p/2m = v/2$ and $v_{\mathrm{g}} = \mathrm{d}\omega/\mathrm{d}k = \mathrm{d}E/\mathrm{d}p = v$, where v is the particle speed.

(16) Prigogine, I.; Lefever, R. *J. Chem. Phys.* **1968**, *48*, 1695.

(17) Dimensionless scaling: $c = k_{\mathrm{f}}/k_3$, $d = k_{\mathrm{b}}/k_3$, $a = k_4/k_3$, $b = k_1/k_3$, where k_1, k_2, k_3, and k_4 are reaction rate constants from the Brusselator scheme.